ADVANCED FUNCTIONAL MATERIALS
www.afm-journal.de



# Hybrid CuTCNQ/AgTCNQ Metal-Organic Charge Transfer Complexes via Galvanic Replacement vs Corrosion-Recrystallization

*Andrew Pearson, Rajesh Ramanathan, Anthony P. O'Mullane,* and Vipul Bansal**

**This study reports a hybrid of two metal-organic semiconductors that are based on organic charge transfer complexes of 7,7,8,8-tetracyanoquinodimethane (TCNQ). It is shown that the spontaneous reaction between semiconducting microrods of CuTCNQ with $Ag^+$ ions leads to the formation of a CuTCNQ/AgTCNQ hybrid, both in aqueous solution and acetonitrile, albeit with completely different reaction mechanisms. In an aqueous environment, the reaction proceeds by a complex galvanic replacement (GR) mechanism, wherein in addition to AgTCNQ nanowires, $Ag^0$ nanoparticles and $Cu(OH)_2$ crystals decorate the surface of CuTCNQ microrods. Conversely, in acetonitrile, a GR mechanism is found to be thermodynamically unfavorable and instead a corrosion-recrystallization mechanism leads to the decoration of CuTCNQ microrods with AgTCNQ nanoplates, resulting in a pure CuTCNQ/AgTCNQ hybrid metal-organic charge transfer complex. While hybrids of two different inorganic semiconductors are regularly reported, this report pioneers the formation of a hybrid involving two metal-organic semiconductors that will expand the scope of TCNQ-based charge transfer complexes for improved catalysis, sensing, electronics, and biological applications.**

## 1. Introduction

Semiconducting charge-transfer complexes of metal-7,7,8,8-tetracyanoquinodimethane (MTCNQ), particularly CuTCNQ and AgTCNQ have the ability to switch from a high to low impedance state upon optical or electrical excitation, which has led to applications of these materials in organic electronics.[1–7] A variety of well-established chemical, electrochemical and photochemical processes may be regularly employed to fabricate pristine MTCNQ structures.[1–7] In recent years, our research efforts have expanded the applicability of MTCNQ nanostructures towards flexible electronics,[8] (photo) catalysis,[6,7,9,10] sensing,[8,11] superhydrophobic surfaces,[12] and antimicrobial fabrics.[13] The newly emerging applications of these traditional organic semiconductors beyond electronics have generated a renewed interest, particularly towards combining MTCNQs with other classes of nanomaterials. The research push in this direction is based on the unprecedented performance of different hybrid materials that is regularly observed over their individual components.[14]

Although fabrication of pristine MTCNQ structures is routinely undertaken, only a select few MTCNQ composites such as those obtained from hybridization with metal oxides,[15] graphene[16] and carbon nanotubes[17] have so far been prepared. Even in these limited recent reports, the final composite is a physical mixture obtained by growing MTCNQ on another material, wherein the original MTCNQ remains unchanged. We recently demonstrated an electroless galvanic replacement (GR) strategy for direct post-synthesis modification of CuTCNQ with Au nanoparticles by reacting CuTCNQ with $[AuBr_4]^-$ ions.[9,10] GR is a powerful approach that is driven by a spontaneous redox reaction between two metal species due to differences in the standard reduction potential of the metal/metal ion couples. Over the past decade, GR mechanisms have been widely applied to create bimetallic nanostructures by exploiting atomic exchange reactions between the metal in the sacrificial template (e.g., $Ag^0$) and the metal ion (e.g., $[AuBr_4]^-$) in solution.[9,10,18]

Our recent work on the GR of CuTCNQ with $[AuBr_4]^-$ ions, for the first time, expanded the scope of GR reactions to non-metallic semiconducting ionic crystals such as $Cu^+TCNQ^-$,[9,10] which was further extended recently to metal oxides.[19] We validated that the GR of CuTCNQ with $[AuBr_4]^-$ ions proceeds via a similar redox mechanism as observed in the case of metal nanocrystals, wherein the pre-existing $Cu^+TCNQ^-$ template undergoes oxidative dissolution into $TCNQ^0$, while $Au^0$ nanoparticles are reductively precipitated onto the CuTCNQ crystals from $[AuBr_4]^-$ ions in the solution.[9,10] We could also establish

Dr. A. Pearson, Dr. R. Ramanathan, Prof. V. Bansal
NanoBiotechnology Research Laboratory
and Ian Potter NanoBioSensing Facility
School of Applied Sciences
RMIT University
GPO Box 2476 V
Melbourne VIC 3001, Australia
E-mail: vipul.bansal@rmit.edu.au
Dr. A. P. O'Mullane
School of Chemistry
Physics and Mechanical Engineering
Queensland University of Technology
GPO Box 2434
Brisbane QLD 4001, Australia
E-mail: anthony.omullane@qut.edu.au

DOI: 10.1002/adfm.201402320

that the solvent in which the GR of CuTCNQ with $[AuBr_4]^-$ ions took place had a significant impact on the mechanism, leading to markedly different reaction products in acetonitrile and water. It was determined that both the solubility and stability of reaction intermediates in the different solvents had significant influences on the GR mechanisms.[9,10]

In the current study, we further expand the scope of GR reactions by investigating the GR of CuTCNQ microcrystals with $Ag^+$ ions independently in acetonitrile and water. The outcomes of these GR reactions were found to be remarkably different than those observed previously employing $[AuBr_4]^-$ ions. For instance, while the GR of CuTCNQ microcrystals with $[AuBr_4]^-$ ions led to the formation of CuTCNQ/Au hybrids;[9,10] a similar reaction with $Ag^+$ ions under otherwise identical conditions resulted in a chemical transformation of CuTCNQ to AgTCNQ, leading to a CuTCNQ/AgTCNQ hybrid material. To the best of our knowledge, a hybrid CuTCNQ/AgTCNQ type material in a single system has not been reported to date. In regards to the solvent effect, in contrast to the previous study with CuTCNQ and $[AuBr_4]^-$ ions where it was found that two different GR mechanisms were operational in water and acetonitrile;[9,10] in the current case involving $Ag^+$ ions, although a GR mechanism was involved in water, a corrosion-recrystallization mechanism was found operative in acetonitrile. While in both these solvents a CuTCNQ/AgTCNQ hybrid metal-organic charge transfer complex material was formed, it was noticed that in water, additional formation of metallic Ag nanoparticles as an impurity phase led to interesting electrical properties, which differed remarkly from the parent CuTCNQ crystals as well as from pure CuTCNQ/AgTCNQ hybrid films.

## 2. Results and Discussion

### 2.1. Synthesis of CuTCNQ in Acetonitrile

Illustrated in **Figure 1** are SEM images of phase I CuTCNQ microrods synthesized through a spontaneous crystallization process in acetonitrile. CuTCNQ microrods with an average cross section of ≈1 μm × 1 μm with faceted corners and 10–20 μm length are observed with a dense coverage across the surface of the Cu foil, which is consistent with our previous studies.[9,10]

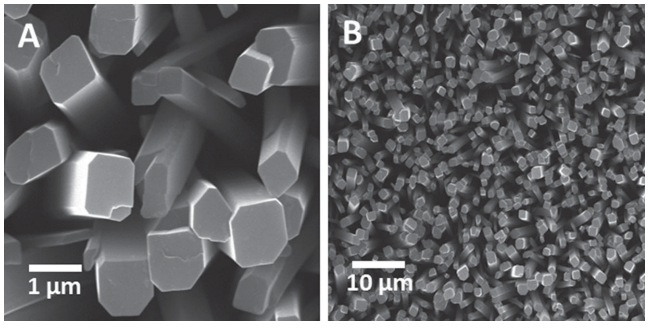


**Figure 1.** SEM images of pristine CuTCNQ microrods synthesized on a copper foil in acetonitrile.

### 2.2. Galvanic Replacement in Aqueous Solution

Illustrated in **Figure 2** and Figure S1 (Supporting Information) are representative SEM images of CuTCNQ galvanically replaced with increasing concentrations of $Ag^+$ ions in aqueous solution. When considering the reaction between CuTCNQ microrods and 1 μM $Ag^+$ ions, we do not observe any dissolution of CuTCNQ microrods, as expected due to the insolubility of CuTCNQ in water,[10] rather we observe the deposition of a small number of large flower-like structures on the topmost faces of the CuTCNQ microrods (Figure 2A). At higher magnification, these structures appear to begin with a single nucleation point and are observed to grow upwards of 1 μm in diameter (Figure S1A). When the concentration of $Ag^+$ ions is increased to 10 μM, the population of flower-like structures on CuTCNQ microrods increases such that they also decorate the sides of the CuTCNQ microrods (Figure 2B). Once again, no dissolution of CuTCNQ is observed. Upon reaction with 50 μM $Ag^+$ ions, we do not observe the same flower-like structures decorating the CuTCNQ microrods (Figure 2C), instead an increasingly roughened surface, which consists of numerous nanowires decorating all the faces of the microrods, is observed (Figure S1C). Increasing the concentration of $Ag^+$ ions to 100 μM results in further decoration of the whole CuTCNQ microrod surface with a large concentration of nanowires (Figure 2D), in addition to large clusters of high aspect ratio nanowires that extend away from the top most faces of the CuTCNQ microrods (Figure S1D). Further increasing the concentration of $Ag^+$ ions to 500 μM enhances the coverage of nanowires, particularly towards the tips of the CuTCNQ microrods (Figure 2E). These high aspect ratio nanowires were found to be of ≈20–30 nm diameter and several tens of micrometers in length (Figure S1E). Reaction with the highest tested 1 mM concentration of $Ag^+$ ions results in large plate-like structures of several micrometers in length along with several smaller nanoparticles decorating the CuTCNQ microrods (Figure 2F). Figure S1F illustrates a CuTCNQ microrod whose surface has been greatly roughened by the deposition of high aspect nanowires and smaller quasi-spherical particles. The formation of nanowires is indicative of AgTCNQ formation as AgTCNQ crystallizes quite readily in nanowire morphology,[17,20] while CuTCNQ mostly crystallizes in a microrod morphology[4,21] and Ag nanoparticles tend to crystallize in a quasi-spherical morphology.[22]

EDX analysis of CuTCNQ microrods reacted with increasing concentrations of $Ag^+$ ions in aqueous solution is shown in **Figure 3**A. Characteristic energy lines of C K$\alpha$ and N K$\alpha$ at 0.277 keV and 0.392 keV, attributed to TCNQ are observed in all samples. All EDX spectra have been normalized to the C K$\alpha$ line as the only source of carbon in the reaction is TCNQ and it is evident later through the proposed mechanism that the total amount of TCNQ species does not change during the reaction. Through increasing the concentration of $Ag^+$ ions in the reaction medium, an increase in the characteristic Ag L$\alpha$ energy line at 3.351 keV is observed indicating an increase in the presence of Ag containing species. Also of note is a slight increase in the characteristic O K$\alpha$ line at 0.524 keV with increasing $Ag^+$ ion concentration, which might be due to potential side reactions involving oxidation of Cu species in water.

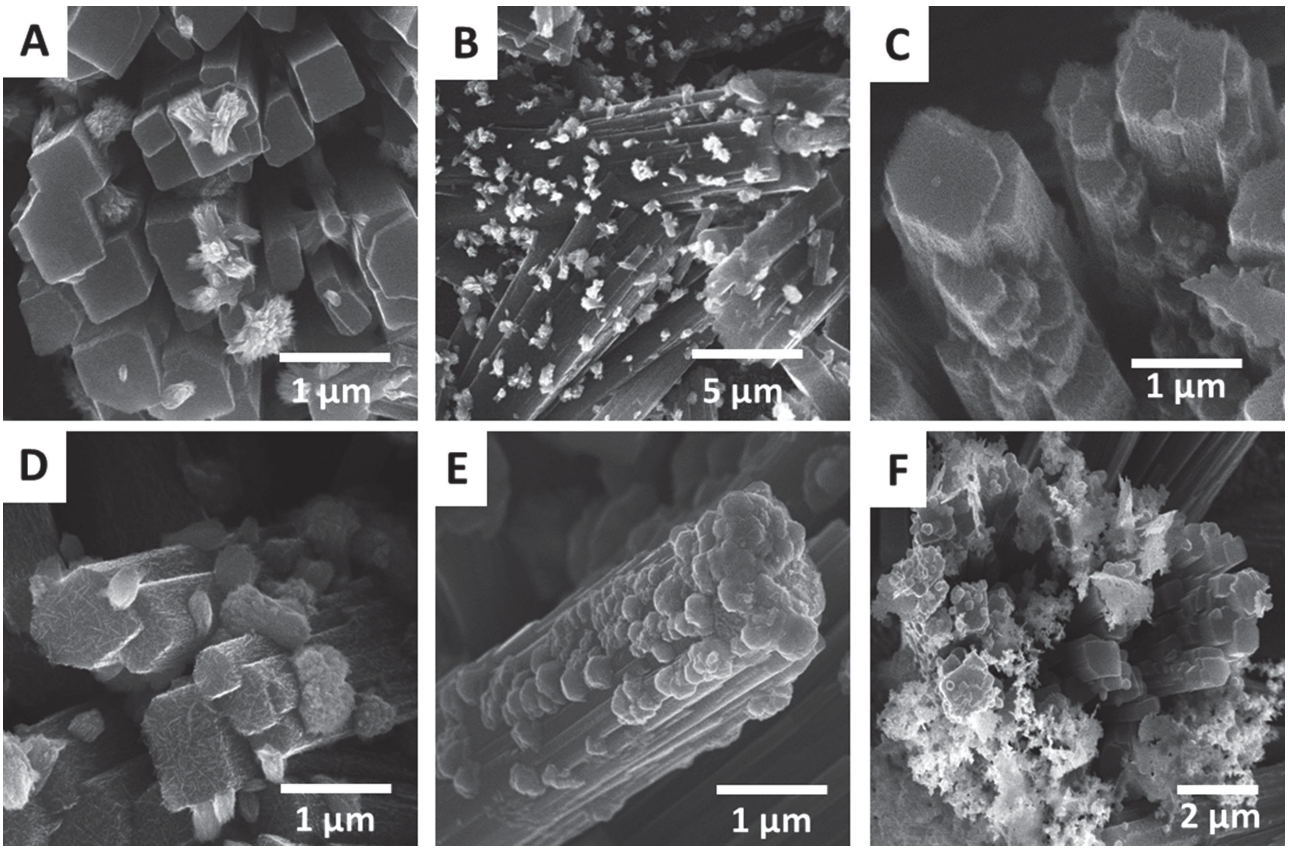


**Figure 2.** SEM images of CuTCNQ microrods galvanically replaced with a) 1 μM, b) 10 μM, c) 50 μM, d) 100 μM, e) 500 μM, and f) 1 mM $Ag^+$ ions in an aqueous solution.

Illustrated in Figure 3B is the Raman spectroscopy analysis of the reaction, which is particularly useful for differentiating between neutral ($TCNQ^0$) or reduced TCNQ ($TCNQ^-$). All spectra except that of pristine $TCNQ^0$ crystals demonstrate features at 1200 $cm^{-1}$ (C = CH bending), 1380 $cm^{-1}$ (C–CN wing stretching), 1600 $cm^{-1}$ (C = C ring stretching) and 2200 $cm^{-1}$

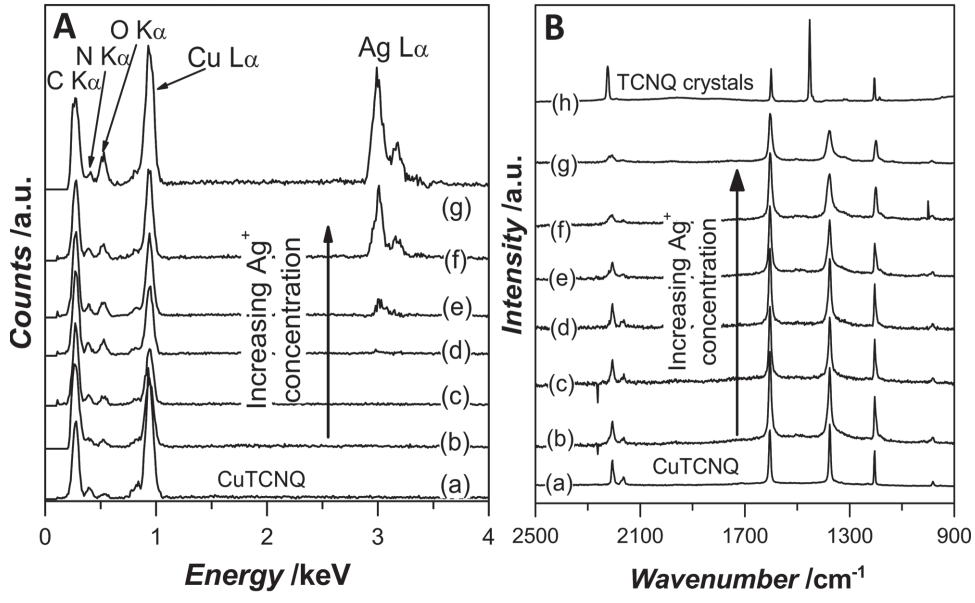


**Figure 3.** A) EDX and B) Raman analysis of CuTCNQ microrods a) before and b–g) after reaction with increasing concentrations of b) 1 μM, c) 10 μM, d) 50 μM, e) 100 μM, f) 500 μM, and g) 1 mM $Ag^+$ ions in aqueous solutions. B-h) Raman spectrum of pristine TCNQ crystals is provided for comparison.

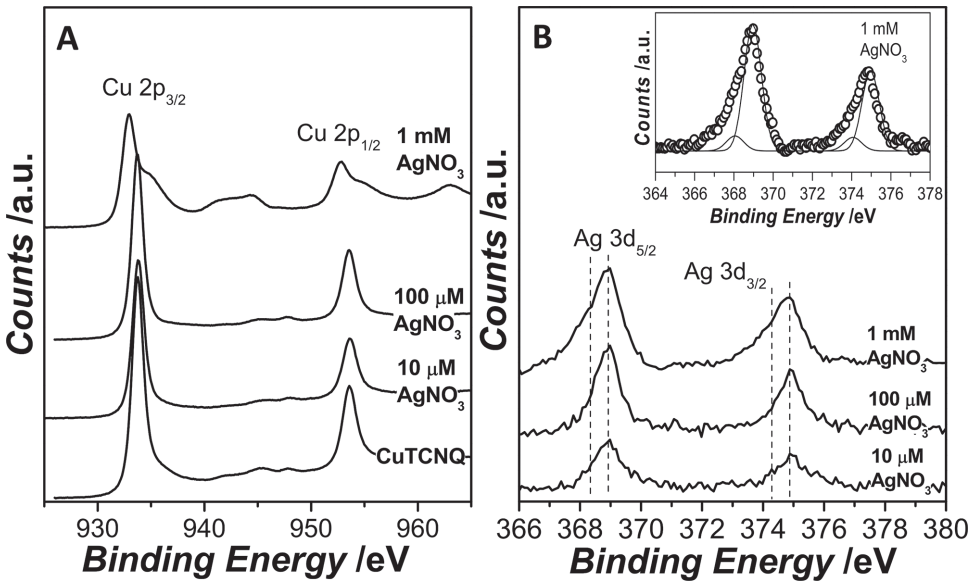


**Figure 4.** XPS spectra showing a) Cu 2p and b) Ag 3d core levels from CuTCNQ microrods before and after their reaction with 10 μM, 100 μM, and 1 mM $Ag^+$ ions in aqueous solutions.

(C–N stretching) confirming the presence of $TCNQ^-$ in all samples, either as CuTCNQ or AgTCNQ.[9,10] Clearly evident is the lack of a noteworthy C–CN wing stretching feature at 1450 $cm^{-1}$ due to $TCNQ^0$, unmistakably indicating that $TCNQ^0$ is not a product of the reaction between CuTCNQ microrods and any concentration of $Ag^+$ ions in aqueous solution.

Cu 2p and Ag 3d core level XPS spectra of the materials synthesized through reaction with 10 μM, 100 μM and 1 mM $Ag^+$ ions in water are displayed in **Figure 4**. Cu 2p core levels of CuTCNQ before and after reaction with 10 μM and 100 μM $Ag^+$ ions show two characteristic $2p_{3/2}$ and $2p_{1/2}$ splitting components at 933.7 eV and 953.7 eV BEs, respectively. Given there are no signatures corresponding to shake-up satellites, it can be confidently concluded that the Cu species in the material is present as $Cu^+$ in CuTCNQ.[9,10,23] However, upon reaction with the highest concentration of 1 mM $Ag^+$ ions, an additional lower BE feature at ≈932.6 eV along with satellite peaks between 940–945 eV is observed. This lower BE along with the presence of shake-up satellite peaks could be attributed to the formation of a $Cu^{2+}$ species due to the formation of $Cu(OH)_2$ in an aqueous reaction environment.[24] This supports the EDX observations that showed an increase in the intensity of O K$\alpha$ with an increase in $Ag^+$ ion concentration, particularly at the 1 mM concentration of $Ag^+$ ions (Figure 3A). The Ag 3d core levels of 10 μM and 100 μM samples could also be split into two characteristic $3d_{5/2}$ and $3d_{3/2}$ components with BE peak maxima at 368.9 eV and 375.0 eV, respectively, supporting the presence of AgTCNQ in these samples.[5,25] Careful examination of the Ag 3d core levels indicates broad peak widths with the Ag 3d spectra skewed towards lower BE. At high $Ag^+$ ion concentration, good signal-to-noise ratio allowed de-convolution of the spectrum (inset, Figure 4B), leading to an additional lower BE $3d_{5/2}$ feature at 368.2 eV that corresponds to metallic Ag.[26] XPS therefore suggests that during GR reactions, while CuTCNQ, AgTCNQ and $Ag^0$ are obtained under all of the tested GR conditions, $Cu(OH)_2$ is formed only at higher concentrations of $Ag^+$ ions.

Since XPS provided evidence for CuTCNQ, AgTCNQ, Ag and $Cu(OH)_2$ species in the reaction products, all of which are crystalline, XRD was employed to validate the XPS observations (**Figure 5**). The XRD pattern of pristine TCNQ crystals displays characteristic signatures of monoclinic TCNQ at 18.6°, 24.2°, 26.0°, 27.5° 28.5°, and 30.1° 2$\theta$ (JCPDS card 00–033–1899). Similarly, pristine CuTCNQ microrods display characteristic XRD peaks at 16.0°, 18.0, 22.5°, 25.0°, and 29.0° 2$\theta$ attributed to the successful formation of phase I CuTCNQ.[3] The XRD pattern of pristine AgTCNQ fabricated on Ag foil is also provided for comparison, which corroborates well with the most commonly obtained phase II AgTCNQ.[3] Reaction of CuTCNQ microrods with increasing concentrations of $Ag^+$ ions in water clearly shows a progressive increase in the intensity of AgTCNQ peaks with a concomitant decrease in CuTCNQ peaks. XRD observations therefore support the microscopy and spectroscopy data suggesting partial chemical transformation of CuTCNQ microrods into AgTCNQ nanowires. Additionally, as expected from the XPS analysis, CuTCNQ reacted with higher concentrations of $Ag^+$ ions, particularly 1 mM, shows the presence of $Ag^0$ nanoparticles along with $Cu(OH)_2$, as evident from peaks marked with (*) and (@), respectively at 37.9° and 61.3° 2$\theta$ for face centered cubic silver (JCPDS 04–0783) and at ≈14.5°, and 34.2° 2$\theta$ for $Cu(OH)_2$ (JCPDS 35–0505). Illustrated in Figure 5B are corresponding XRD patterns in the 55–65° 2$\theta$ region that further affirm the XPS observations that $Ag^0$ is formed at all of the $Ag^+$ ion concentrations employed in these experiments.

Based on the microscopy and spectroscopy findings discussed above, a plausible mechanism for the GR of CuTCNQ with increasing concentrations of $Ag^+$ ions in aqueous solutions may be proposed (**Scheme 1**). First and foremost, consideration must be given to the solubility of CuTCNQ and AgTCNQ in aqueous solution. Both are highly insoluble in water and therefore dissolution of CuTCNQ and AgTCNQ during the reaction is unlikely.[27] Initially, step 1 involves a GR reaction between CuTCNQ microrods and $Ag^+$ ions via Equation 1:

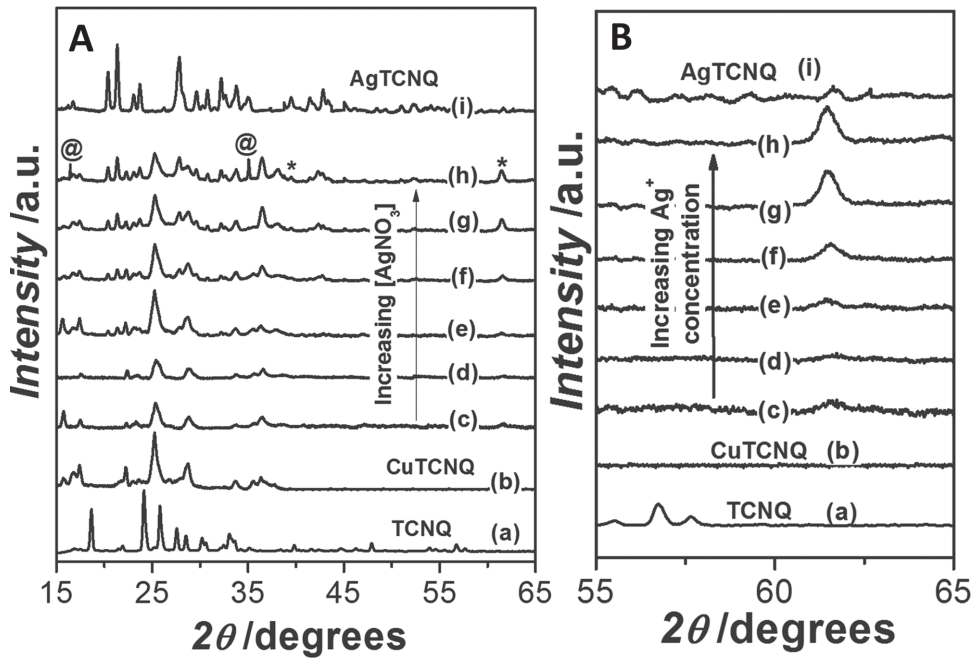


**Figure 5.** A) XRD patterns of a) pristine TCNQ crystals, b) pristine CuTCNQ microrods, c–h) CuTCNQ microrods reacted with c) 1 μM, d) 10 μM, e) 50 μM, f) 100 μM, g) 500 μM, h) 1 mM $AgNO_3$ in aqueous solutions, and i) pristine AgTCNQ. B) As in (A) but showing only the 55–65° 2$\theta$ region to reflect the presence of $Ag^0$ at all the reaction conditions.

$$CuTCNQ_{(s)} + AgNO_{3(aq)} \rightarrow Ag^0_{(s)} + Cu^+_{(aq)} + TCNQ^0_{(s)} + NO^-_{3(aq)} \quad (1)$$

We previously demonstrated that the reaction between CuTCNQ microrods and $[AuBr_4]^-$ ions in aqueous solutions proceeds via a GR mechanism, as CuTCNQ oxidizes over the potential range of +0.5–0.7 V (vs SHE), whereas the standard reduction potential for the $[AuBr_4]^-/Au^0$ couple is +0.854 V (vs SHE).[9] Similarly, the GR of CuTCNQ microrods with $Ag^+$ ions will also be thermodynamically possible in aqueous solution due to the standard reduction potential for the $Ag^+/Ag^0$ couple being ≈0.8 V (vs SHE). Following the GR reaction, steps 2–6 are expected to occur simultaneously, however these are divided for the ease of discussion. To start with, the possibility of reaction between newly generated $Cu^+$ ions via CuTCNQ oxidation and $Ag^+$ ions can be discounted as $Cu^+$ species are unstable and prone to spontaneous disproportionation

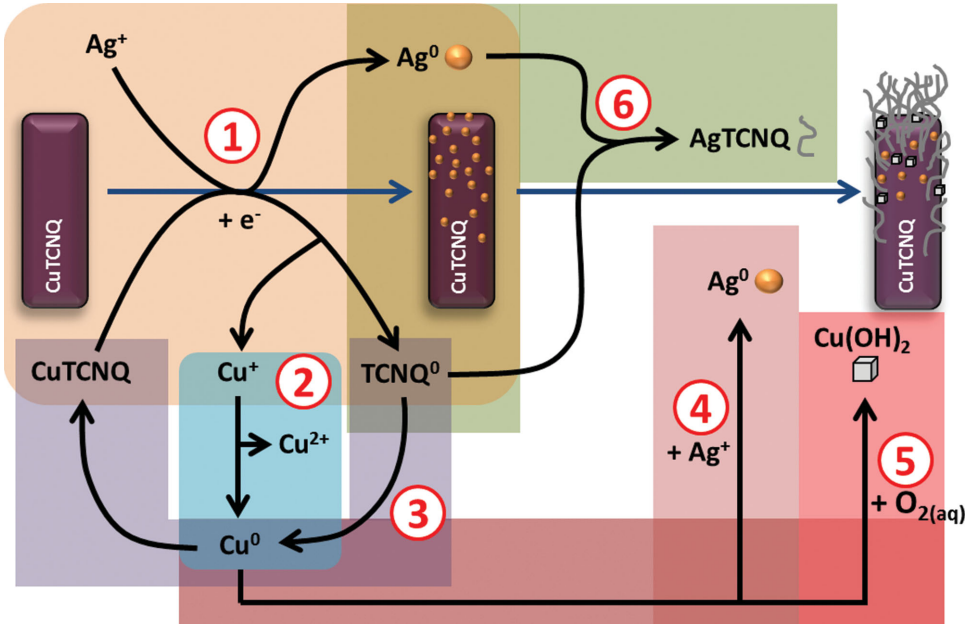


**Scheme 1.** Reaction between CuTCNQ microrods and $Ag^+$ ions in an aqueous solution.

in aqueous solution to form $Cu^0$ and $Cu^{2+}$ via Equation 2 (step 2):[9,28]

$$2Cu^{+}_{(aq)} \rightleftharpoons Cu^{2+}_{(aq)} + Cu^{0}_{(s)} \quad (2)$$

While it is thermodynamically possible that $Ag^+$ ions may react with $Cu^+$ ions in aqueous solution ($Cu^+/Cu^{2+}$ +0.159 V vs SHE), the extremely fast rate of the disproportionation reaction will mean that even if this reaction happens, only a negligible proportion of $Cu^+$ ions may react with $Ag^+$ ions. Therefore we propose that this side reaction will have minimal impact on the proposed mechanism.

The $Cu^0$ species generated through the disproportionation reaction is now able to react in a number of different ways, as is shown by steps 3–5. It is known that in aqueous solution, $Cu^0$ can spontaneously react with $TCNQ^0$.[29] In the current case, as shown in step 3 and Equation 3, $Cu^0$ produced via Equation 2 reacts with $TCNQ^0$ produced via Equation 1 to regenerate some of the CuTCNQ that was originally oxidized during the GR reaction:

$$Cu^{0}_{(s)} + TCNQ^{0}_{(s)} \rightleftharpoons CuTCNQ_{(s)} \quad (3)$$

The above reaction is supported by the absence of TCNQ° C–CN wing stretching signatures in the Raman study, indicating that all of the $TCNQ^0$ generated during the GR reaction is consumed either through CuTCNQ regeneration or through transformation into AgTCNQ. This also agrees well with the SEM images that show little or no change in the size or morphology of the underlying CuTCNQ microrods during the GR reaction.

In addition to Equation 3, $Cu^0$ may also undergo a spontaneous GR reaction with $Ag^+$ ions to form $Ag^0$ during step 4 and be oxidized in an aqueous oxygen-rich environment to form $Cu(OH)_2$ during step 5, as shown via Equation 4:

$$Cu^{0}_{(s)} + 2Ag^{+}_{(aq)} + \frac{1}{2}O_{2_{(aq)}} + H_2O \rightarrow Cu(OH)_{2_{(s)}} + 2Ag^{0}_{(s)} \quad (4)$$

Formation of small amounts of $Ag^0$ nanoparticles and $Cu(OH)_2$ during the GR reaction were indeed noticed during XPS, XRD and SEM analysis of samples, thereby supporting the above reaction. While $Cu^+$ species released via oxidation of CuTCNQ during the GR reaction leads to different products such as $Cu^0$, $Cu^{2+}$, $Cu(OH)_2$ and regenerated CuTCNQ, the $Ag^0$ species formed in-parallel via reduction of $Ag^+$ ions through steps 1 and 4 is also available to undergo further reaction with $TCNQ^0$ as outlined in Step 6. Similar to $Cu^0$ and $TCNQ^0$ in aqueous solution, $Ag^0$ and $TCNQ^0$ can also react spontaneously to form AgTCNQ, as described via Equation 5:

$$Ag^{0}_{(s)} + TCNQ^{0}_{(s)} \rightleftharpoons AgTCNQ_{(s)} \quad (5)$$

As some of the $TCNQ^0$ is consumed during reaction with $Cu^0$ during CuTCNQ regeneration (Equation 3), not all of the $Ag^0$ produced during the reaction may be able to react with $TCNQ^0$, thereby leading to decoration of CuTCNQ microrods with Ag nanoparticles. A combination of reactions discussed through Equations 1–5 lead to a hybrid CuTCNQ/AgTCNQ material that seems to be contaminated with $Ag^0$ nanoparticles as well as $Cu(OH)_2$, however not all of these reactions are likely to proceed at the same rate. To gain further understanding of the reaction mechanism in water, three stoichiometric possibilities, wherein the overall reaction is either favored towards AgTCNQ or CuTCNQ formation or towards an intermediate possibility, may be considered (Figure S2–S4, Supporting Information). It may be noted that these possibilities also take the stoichiometric formation of water-soluble $Cu(NO_3)_2$ into account that was not discussed so far, as focus was only on those reactions that occurred on the solid CuTCNQ surface.

As the first possibility, let us consider a scenario wherein the overall reaction is favored towards CuTCNQ regeneration (Equation 3). It may be expected that as $TCNQ^0$ and $Cu^0$ are initially generated on the CuTCNQ surface in close proximity to each other, the majority of $Cu^0$ reacts with $TCNQ^0$, with this reaction being limited by the regeneration rate of CuTCNQ. As illustrated from Figure S2 (Supporting Information), even in this case, only a maximum of 50% CuTCNQ oxidized during the GR reaction could be regenerated, while an equivalent amount of AgTCNQ and $Ag^0$ is produced and no $Cu(OH)_2$ is produced. Even though the reaction did not lead to the formation of $Cu(OH)_2$ directly on the CuTCNQ surface, a soluble $Cu^{2+}$ species, most likely $Cu(NO_3)_2$ is still formed during the reaction. This soluble $Cu^{2+}$ species may be washed off from the CuTCNQ surface during sample cleaning before characterization. This is in fact evident from GR reactions at lower $Ag^+$ ion concentrations, wherein $Cu(OH)_2$ as well as no other $Cu^{2+}$ species is detected as the reaction product. This suggests that at low $Ag^+$ ion concentration, the recombination rate of $Cu^0$ and $TCNQ^0$ to regenerate CuTCNQ is able to keep pace with the GR reaction.

However, when the concentration of $Ag^+$ ions is increased significantly, signatures corresponding to $Cu(OH)_2$ are seen, indicating that the reaction shown in Equation 4 only occurs when high concentration of $Ag^+$ ions causes the rate of AgTCNQ formation to exceed the rate of CuTCNQ regeneration. This is illustrated from Figure S3 (Supporting Information) that considers a scenario where the overall reaction is dominated by AgTCNQ formation. As evident from Equation 1, $Ag^0$ and $TCNQ^0$ are generated simultaneously in close proximity to each other on the surface of CuTCNQ microrods, which can react together to form AgTCNQ via Equation 5. It is also imperative that if all of the $TCNQ^0$ is consumed through reaction with $Ag^0$ (Equation 5), no $TCNQ^0$ will be available to react with $Cu^0$ to form CuTCNQ (Equation 3) and as a result the side reactions leading to $Cu(OH)_2$ formation will dominate. The experimental outcomes suggest that with the increasing concentration of $Ag^+$ ions during the GR reaction, the reaction equilibrium in fact shifts in this direction, leading to an increasing presence of $Cu(OH)_2$ crystals and AgTCNQ nanowires on the surface of CuTCNQ microrods. In this case, the overall reaction is limited by the rate of AgTCNQ formation. While it is shown in Figure S3 that the final product of such reaction will be AgTCNQ and $Cu(OH)_2$ without any $Ag^0$ formation, since the rate of CuTCNQ formation is typically much faster than AgTCNQ formation,[6] the reaction possibility shown in Figure S3 cannot operate in isolation. This is supported by the presence of high amounts of $Ag^0$ on CuTCNQ at high $Ag^+$ ion concentration, which is not a reaction outcome in this proposed scenario.

This suggests that the final product obtained through the GR of CuTCNQ with $Ag^+$ ions in water relies on a complex interplay between different competing reactions, such that the occurrence of one reaction has a significant effect on the likelihood of another. Figure S4 (Supporting Information) considers a scenario that is closest to the actual reaction, in which different reactions have different levels of probability. It may be noticed that in such a case, while AgTCNQ is the predominant reaction product, all other products experimentally observed in this study such as CuTCNQ, $Cu(OH)_2$ and $Ag^0$ are also formed. Therefore, on the basis of three proposed scenarios, it is clear that the GR reaction between CuTCNQ and $Ag^+$ ions in water will always lead to a CuTCNQ/AgTCNQ hybrid that is contaminated with $Ag^0$ nanoparticles, but may or may not be contaminated with $Cu(OH)_2$ depending on the $Ag^+$ ion concentration used.

### 2.3. Reaction Between CuTCNQ and $AgNO_3$ in Acetonitrile Solution

Since MTCNQs have high solubility in acetonitrile (0.14 ± 0.04 mM for CuTCNQ and 0.15 ± 0.02 mM for AgTCNQ),[2] in contrast to almost no solubility in water, reaction between CuTCNQ and increasing concentrations of $Ag^+$ ions was also investigated in acetonitrile. Unlike the reaction in water, which follows a GR mechanism, the potential of the $Ag^+/Ag^0$ couple in acetonitrile (+0.318 V vs SHE)[2] has insufficient driving force to oxidize CuTCNQ (+0.5–0.7 V vs SHE).[29] However, as evident from SEM images in **Figure 6** and Figure S5 (Supporting Information), we still observe the growth of intricate structures on the surface of the CuTCNQ microrods. CuTCNQ microrods, when reacted with 1 μM $Ag^+$ ions in acetonitrile, undergo a hollowing process with the resultant microtubes possessing ≈200 nm thick roughened side walls (Figure 6A and Supporting Information Figure S5A). Interestingly, the diameter of the CuTCNQ microrods is observed to increase from 1.0 μm originally to 1.5–2.0 μm post-hollowing. This suggests that CuTCNQ initially dissolves from the top-most faces of the microrods into $Cu^+$ and $TCNQ^-$ ions in a manner analogous to pitting corrosion, which is followed by crystallization of $Ag^+$ and $TCNQ^-$ to form AgTCNQ on the outer surface of the CuTCNQ microtubes. We have previously documented the formation of hollow CuTCNQ microtubes through a competing corrosion-crystallization process when CuTCNQ microrods were reacted with a similar concentration of $[AuBr_4]^-$ ions in acetonitrile.[10] However, in the previous study, the $[AuBr_4]^-$ ions had a sufficiently positive reduction potential to drive the GR reaction with CuTCNQ in acetonitrile, which is not the case with $Ag^+$ ions. This led to a completely different set of reaction products and a different reaction mechanism in the previous study.

In the current study, when CuTCNQ is exposed to a higher concentration (10 μM) of $Ag^+$ ions, the hollowing out of

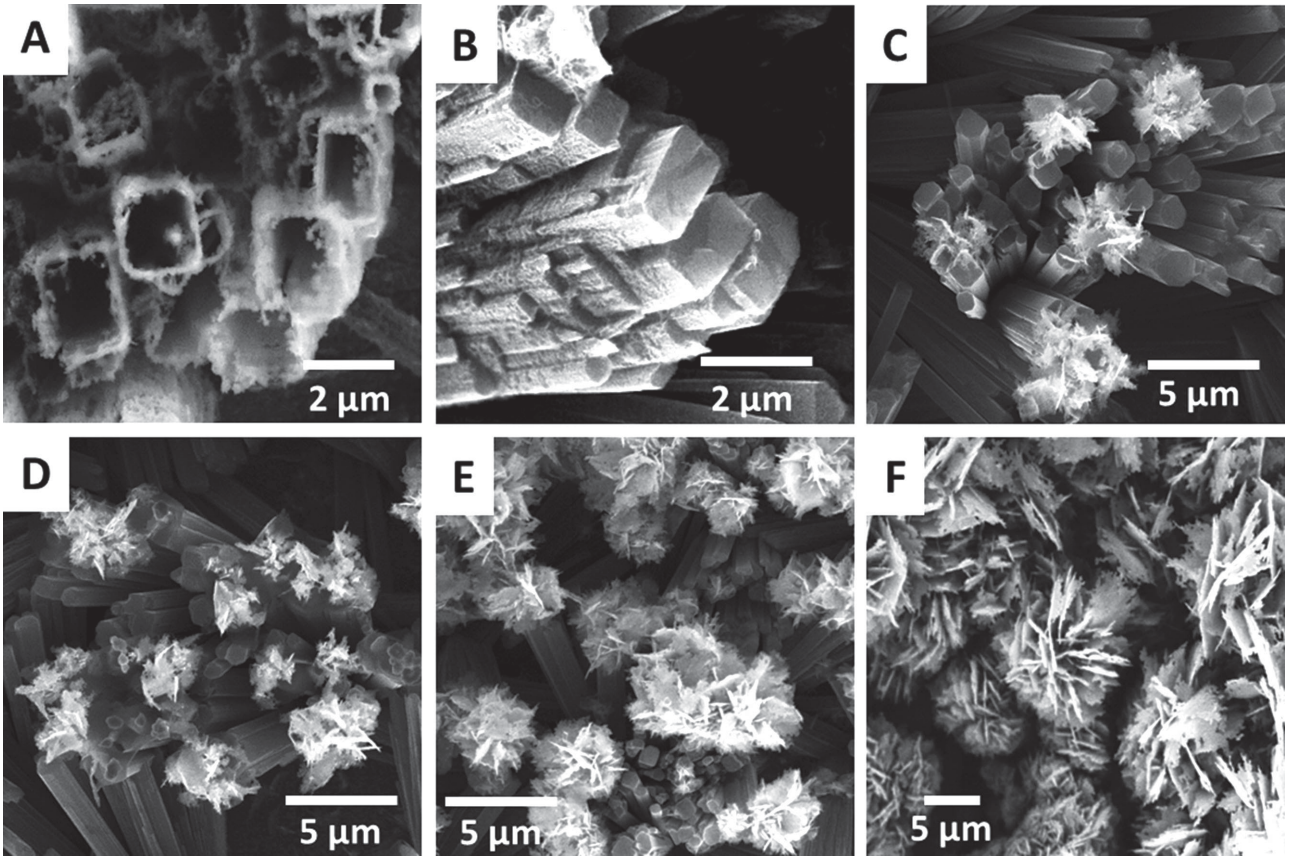


**Figure 6.** SEM images of CuTCNQ microrods galvanically replaced with a) 1 μM, b) 10 μM, c) 50 μM, d) 100 μM, e) 500 μM, and f) 1 mM $Ag^+$ ions in acetonitrile solution.

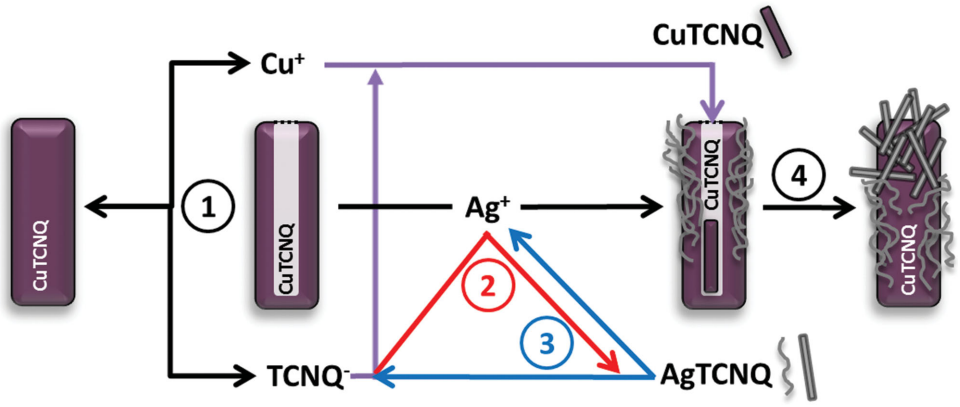


**Scheme 2.** Reaction between CuTCNQ microrods and $Ag^+$ ions in acetonitrile.

CuTCNQ microrods is no longer observed and the microrods maintain their original diameter of ≈1 µm. However, a similar roughening of the side walls is still observed (Figure 6B). The higher magnification SEM image of the side wall shows thin nanowire-like structures, which may be attributed to AgTCNQ based on its preferred morphology (Figure S5B, Supporting Information). A further increase in the concentration of $Ag^+$ ions to 50 µM through 100 µM, 500 µM, and 1 mM (Figure 6C–F, respectively) results in hybrid structures with similar morphologies. In each case, clusters of plate-like structures are observed on the top-most faces of CuTCNQ microrods, which increase in density, plate size and plate thickness with the increasing concentration of $Ag^+$ ions (50 µM < 100 µM < 500 µM < 1 mM).

In stark contrast to the GR reaction observed between CuTCNQ and $Ag^+$ ions in water, we propose that in acetonitrile CuTCNQ does not undergo GR reaction with $Ag^+$ ions (**Scheme 2**). Instead, in acetonitrile, AgTCNQ is formed on CuTCNQ surface through a spontaneous crystallization reaction between $Ag^+$ ions as reactant and $TCNQ^-$ ions liberated in situ from the dissolution of CuTCNQ via Equation 6,7:

$$CuTCNQ_{(s)} \rightleftharpoons Cu^+ + TCNQ^- \quad (6)$$

$$Ag^+ + TCNQ^- \rightleftharpoons AgTCNQ_{(s)} \quad (7)$$

At the initial stages of reaction, as CuTCNQ is the sole species present in acetonitrile, the initial rate of dissolution (forward reaction in Equation 6 is likely to be high as per Le Chateliers principle. Furthermore, as the concentrations of both $Cu^+$ and $TCNQ^-$ ions increase in acetonitrile, the reverse reaction of Equation 6, the CuTCNQ re-crystallization will also proceed. This spontaneous corrosion-crystallization will continue until both processes reach equilibrium (step 1). Upon introduction of $Ag^+$ ions to this system, spontaneous crystallization between $Ag^+$ and $TCNQ^-$ ions to form solid AgTCNQ (Equation 7) will compete with that of CuTCNQ (reverse of Equation 6) until equilibrium is achieved (step 2). The existing CuTCNQ microrods will act as preferred nucleation sites for the growth of AgTCNQ nanowires. Notably, the solid AgTCNQ formed on the surface of CuTCNQ will itself be prone to dissolution in acetonitrile (step 3) via Equation 8:

$$AgTCNQ_{(s)} \rightleftharpoons Ag^+ + TCNQ^- \quad (8)$$

Significantly, as the concentration of $TCNQ^-$ decreases upon reaction with $Ag^+$ (Equation 7), the dissolution of both CuTCNQ (Equation 6) and AgTCNQ (Equation 8) will simultaneously increase to equilibrate the concentration of $TCNQ^-$ in the reaction medium. Eventually, these reactions reach equilibrium where the rate of crystallization is equal to the rate of dissolution of all the species (step 4). Therefore, the final product of the reaction between $Ag^+$ ions and CuTCNQ in acetonitrile will be a hybrid CuTCNQ/AgTCNQ material, in which the relative proportions of CuTCNQ and AgTCNQ will be dictated by the rates of spontaneous co-crystallization and co-dissolution of AgTCNQ and CuTCNQ as well as the amount of $Ag^+$ ions introduced to the reaction. At the lowest $Ag^+$ ion concentration (1 µM), we observe the formation of hollow CuTCNQ/AgTCNQ microrods, wherein the majority of the hybrid is CuTCNQ, whereas at highest $Ag^+$ ion concentration (1 mM), the majority of the hybrid material transforms into AgTCNQ. The outcomes of Raman spectroscopy, UV–Visible absorbance spectroscopy, XPS and XRD analyses of reactions between CuTCNQ and $Ag^+$ ions in acetonitrile are discussed in Supporting Information that endorse the above-proposed reaction mechanism (Figure S6–S9, Supporting Information).

### 2.4. Electrical Conductivity of CuTCNQ/AgTCNQ Hybrids Obtained via Galvanic Replacement vs Corrosion-Recrystallization

It is clear that the GR reaction between CuTCNQ and $Ag^+$ ions in water leads to a complex hybrid that is comprised of CuTCNQ/AgTCNQ/Ag/$Cu(OH)_2$, whereas the corrosion-recrystallization mechanism in acetonitrile leads to a pure CuTCNQ/AgTCNQ hybrid without other contaminant species. While both AgTCNQ and CuTCNQ show semiconducting behavior, AgTCNQ is known for its significantly lower conductivity (≈2.48 × $10^{-3}$ S $cm^{-1}$) and charge carrier mobility (≈6.49 × $10^{-6}$ $cm^2$ $V^{-1}$ $s^{-1}$) compared to CuTCNQ (≈2 S $cm^{-1}$; 5.34 × $10^{-3}$ $cm^2$ $V^{-1}$ $s^{-1}$).[30] This suggests that in acetonitrile, where a pure CuTCNQ/AgTCNQ hybrid is formed, the electrical conductivity of the hybrid must be reduced with the

increasing concentration of the $Ag^+$ ion. This is in fact evident from Figure S10 (Supporting Information), which shows a consistent increase in the resistance of the CuTCNQ/AgTCNQ hybrid films prepared in acetonitrile over that of pristine CuTCNQ film under identical measurement conditions, when the AgTCNQ fraction of the hybrid film is increased. Conversely, the CuTCNQ/AgTCNQ/Ag/$Cu(OH)_2$ hybrid films obtained in water show a consistent decrease in the resistance over that of pristine CuTCNQ film with increasing $Ag^+$ ions concentration. This increase in film conductivity obtained in water is most likely due to the presence of metallic Ag nanoparticles on the surface of the CuTCNQ/AgTCNQ hybrid, which were found absent in acetonitrile. This difference in conductivity behavior not only further supports the proposed mechanisms involved during the reaction between CuTCNQ and $Ag^+$ ions; it also signifies the importance of reaction conditions and the role of minor impurity phases in dictating the final properties of nanomaterials.

## 3. Conclusion

This study, for the first time, demonstrates the feasibility of fabricating hybrids of two metal-organic charge transfer complexes ($M_1$TCNQ/$M_2$TCNQ) by a facile route involving immersion of pre-existing $M_1$TCNQ in a suitable metal ion ($M_2$) solution. The outcomes of this study support a recent observation by Nafady and co-workers that investigated the competition between $Ni^{2+}$ and $Co^{2+}$ insertion into TCNQ under electrochemical conditions where both cations were accommodated under an appropriate applied potential and precursor concentrations.[31] The current study specifically demonstrated the fabrication of a CuTCNQ/AgTCNQ hybrid by a simple reaction between CuTCNQ with $Ag^+$ ions, independently in water and in acetonitrile. Detailed mechanistic investigations of these reactions show that in aqueous solutions, the reaction mechanism is quite complex that involves a spontaneous GR reaction between CuTCNQ microrods and $Ag^+$ ions, along with co-crystallization of CuTCNQ and AgTCNQ. This results in the formation of CuTCNQ microrods decorated with AgTCNQ nanowires, in addition to Ag nanoparticles and $Cu(OH)_2$ crystals contaminating the CuTCNQ/AgTCNQ surface. Conversely, when the same reaction is performed in acetonitrile, the reaction is unable to proceed via a GR mechanism and instead a relatively simple corrosion-recrystallization mechanism is involved. Therefore, in acetonitrile, a pure CuTCNQ/AgTCNQ hybrid material comprised of CuTCNQ microrods decorated with AgTCNQ nanoplates is obtained, which is found not to be contaminated with Ag nanoparticles or $Cu(OH)_2$. The comparison of electrical conductivities of CuTCNQ/AgTCNQ hybrid films fabricated in these two solvents revealed an interesting behavior. The presence or absence of contaminant species in films formed in water or acetonitrile, respectively, impacted the conductivity of the hybrid films via an increase or decrease, respectively, over that of a pristine CuTCNQ film. These unique characteristics of these hybrid materials may make them suitable for different applications. Futhermore, it may be noted that since the reaction mechanism in acetonitrile does not involve a GR mechanism, and instead involves a corrosion-recrystallization mechanism, it is highly likely that acetonitrile-based reactions may offer a more general strategy to prepare a variety of $M_1$TCNQ/$M_2$TCNQ type hybrid metal-organic charge transfer complexes. Although TCNQ-based metal-organic charge transfer complexes have been actively explored in the past for a variety of electronic applications, this study not only provides the first account of the chemical synthesis of a hybrid $M_1$TCNQ/$M_2$TCNQ material in the literature, it does so while obtaining deep mechanistic understanding of their formation. A generalized approach to produce metal-organic semiconductor hybrids and heterojunctions in a facile manner is likely to fuel a renewed interest in the field. This work will lay the foundation of our future research on fabrication of a variety of hybrid $M_1$TCNQ/$M_2$TCNQ metal-organic charge transfer complexes and their new biological, catalytic and electronic applications.

## 4. Experimental Section

*Materials*: Copper (99% purity) and silver (99% purity) foils were obtained from Chem Supply; 7,7,8,8-tetracyanoquinodimethane (TCNQ) was obtained from Fluka; silver nitrate ($AgNO_3$) was obtained from Sigma-Aldrich; and acetonitrile was obtained from BDH Chemicals. Copper and silver foils were treated with dilute nitric acid (Sigma-Aldrich), rinsed with deionized water (MilliQ) and dried with a flow of $N_2$ gas prior to use. All other chemicals were used as received.

*Synthesis of CuTCNQ and AgTCNQ in Acetonitrile*: A 20 cm × 1.5 cm × 0.015 cm strip of copper foil was placed in 50 mL of 5 mM TCNQ solution in acetonitrile for 1 h. The surface of the copper foil was observed to turn dark purple, indicating the formation of CuTCNQ. The CuTCNQ foil was then washed three times with deionized water and dried under $N_2$ gas. The CuTCNQ foil was cut into multiple 1.5 cm × 1.5 cm pieces to ensure that all subsequent experiments were performed on the same batch of CuTCNQ. As a control experiment, a 1.5 cm × 1.5 cm × 0.020 cm piece of silver foil was immersed in 10 mL of a 5 mM TCNQ solution in acetonitrile for 1 h. The surface of the Ag foil turned into a blue/purple color indicating the formation of AgTCNQ.[3] The AgTCNQ foil was washed with deionized water and dried under $N_2$ gas.

*Reaction between CuTCNQ and $AgNO_3$ in Water and Acetonitrile*: Two sets of experiments were performed simultaneously in acetonitrile and water. Six pieces of CuTCNQ synthesized in acetonitrile were each added to separate solutions containing increasing concentrations of $AgNO_3$ (1 μM, 10 μM, 50 μM, 100 μM, 500 μM, 1 mM) in 5 mL of acetonitrile or water and allowed to react for 4 h. CuTCNQ foils were removed from their respective solutions and thoroughly washed with deionized water to remove any unconsumed reagents and/or soluble products. The materials were then examined using scanning electron microscopy (FEI NovaSEM), energy dispersive X-rays (EDX was performed on an FEI NovaSEM coupled with EDX Si(Li) X-ray detector), X-ray photoelectron spectroscopy (XPS – Thermo K-Alpha XPS operating at a pressure better than $1 \times 10^{-9}$ Torr with core levels aligned to C 1s binding energy (BE) of 285 eV), X-ray diffraction (XRD – Bruker AXS D8 Discover with General Area Detector Diffraction System using Cu K$\alpha$ irradiation: $\lambda$ = 0.15418 nm) and Raman spectroscopy (Perkin Elmer Raman Station 200F). Electrical conductivity measurements on pristine CuTCNQ films and hybrid CuTCNQ/AgTCNQ films fabricated on Cu substrates in water and acetonitrile were performed using an Agilent 2912A sourcemeter while employing microelectrodes (100 μm tip diameter) that were placed directly on the films at equal distance during two-probe direct current measurements. The relative change in conductivity was plotted as a change in resistance of the hybrid CuTCNQ/AgTCNQ films over that of pristine CuTCNQ film.

## Supporting Information

Supporting Information is available from the Wiley Online Library or from the author.

## Acknowledgements

The Australian Research Council is acknowledged for Future Fellowships awarded to V.B. (FT140101285) and A.O.M. (FT110100760). V.B. acknowledges the generous support of the Ian Potter Foundation in establishing a multimode spectroscopy facility and Ian Potter NanoBioSensing Facility at RMIT University. The authors thank Dr. Sumeet Walia to assist with conductivity measurements while acknowledging the instrument and technical support of RMIT Microscopy and Microanalysis Facility.

Received: July 13, 2014
Revised: September 9, 2014
Published online: October 6, 2014

[1] a) A. Nafady, A. P. O'Mullane, A. M. Bond, *Coord. Chem. Rev.* **2014**, *268*, 101; b) L. Shields, *J. Chem. Soc., Faraday Trans. II: Mol. Chem. Phys.* **1985**, *81*, 1; c) H. Miyasaka, N. Motokawa, S. Matsunaga, M. Yamashita, K. Sugimoto, T. Mori, N. Toyota, K. R. Dunbar, *J. Am. Chem. Soc.* **2010**, *132*, 1532; d) E. B. Vickers, T. D. Selby, M. S. Thorum, M. L. Taliaferro, J. S. Miller, *Inorg. Chem.* **2004**, *43*, 6414; e) A. P. O'Mullane, A. K. Neufeld, A. R. Harris, A. M. Bond, *Langmuir* **2006**, *22*, 10499; f) A. Nafady, A. M. Bond, A. Bilyk, A. R. Harris, A. I. Bhatt, A. P. O'Mullane, R. De Marco, *J. Am. Chem. Soc.* **2007**, *129*, 2369; g) A. P. O'Mullane, N. Fay, A. Nafady, A. M. Bond, *J. Am. Chem. Soc.* **2007**, *129*, 2066; h) A. Nafady, A. M. Bond, A. P. O'Mullane, *Inorg. Chem.* **2009**, *48*, 9258; i) R. Muller, J. Genoe, P. Heremans, *Appl. Phys. Lett.* **2006**, *88*; j) H. Liu, Z. Liu, X. Qian, Y. Guo, S. Cui, L. Sun, Y. Song, Y. Li, D. Zhu, *Cryst. Growth Des.* **2009**, *10*, 237; k) K. Xiao, I. N. Ivanov, A. A. Puretzky, Z. Liu, D. B. Geohegan, *Adv. Mater.* **2006**, *18*, 2184; l) H. Duan, D. O. Cowan, J. Kruger, *J. Electrochem. Soc.* **1993**, *140*, 2807.

[2] A. R. Harris, A. Nafady, A. P. O'Mullane, A. M. Bond, *Chem. Mater.* **2007**, *19*, 5499.

[3] a) R. A. Heintz, H. Zhao, X. Ouyang, G. Grandinetti, J. Cowen, K. R. Dunbar, *Inorg. Chem.* **1999**, *38*, 144; b) S. A. O'Kane, R. Clerac, H. Zhao, X. Ouyang, J. R. Galan-Mascaros, R. Heintz, K. R. Dunbar, *J. Solid State Chem.* **2000**, *152*, 159.

[4] A. K. Neufeld, A. P. O'Mullane, A. M. Bond, *J. Am. Chem. Soc.* **2005**, *127*, 13846.

[5] C.-W. Yuan, C.-R. Wu, Y. Wei, W.-Y. Yang, *Thin Solid Films* **1994**, *243*, 679.

[6] A. Pearson, V. Bansal, A. P. O'Mullane, *Electrochim. Acta* **2013**, *114*, 189.

[7] A. Pearson, A. P. O'Mullane, *ChemPlusChem* **2013**, *78*, 1343.

[8] R. Ramanathan, A. E. Kandjani, S. Walia, S. Balendhran, S. K. Bhargava, K. Kalantar-zadeh, V. Bansal, *RSC Adv.* **2013**, *3*, 17654.

[9] A. Pearson, A. P. O'Mullane, S. K. Bhargava, V. Bansal, *Inorg. Chem.* **2012**, *51*, 8791.

[10] A. Pearson, A. O'Mullane, S. K. Bhargava, V. Bansal, *Inorg. Chem.* **2011**, *50*, 1705.

[11] R. Ramanathan, S. Walia, A. E. Kandjani, S. Balendhran, M. Mohammadtaheri, S. K. Bhargava, K. Kalantar-zadeh, V. Bansal, Langmuir **2014**, DOI: 10.1021/la501446b.

[12] M. Mahajan, S. K. Bhargava, A. O'Mullane, *Electrochim. Acta* **2012**, *101*, 186.

[13] Z. M. Davoudi, A. E. Kandjani, A. I. Bhatt, I. L. Kyratzis, A. P. O'Mullane, V. Bansal, *Adv. Funct. Mater.* **2014**, *24*, 1047.

[14] a) H. Lin, H. Liu, X. Qian, S. Chen, Y. Li, Y. Li, *Inorg. Chem.* **2013**, *52*, 6969; b) O. Mishima, J. Tanaka, S. Yamaoka, O. Fukunaga, *Science* **1987**, *238*, 181; c) K. Wang, X. Qian, L. Zhang, Y. Li, H. Liu, *ACS Appl. Mater. Interfaces* **2013**, *5*, 5825; d) W. Zhang, W. Jin, T. Fukushima, A. Saeki, S. Seki, T. Aida, *Science* **2011**, *334*, 340.

[15] a) H. Liu, S. Cui, Y. Guo, Y. Li, C. Huang, Z. Zuo, X. Yin, Y.-Y. Song, D. Zhu, *J. Mater. Chem.* **2009**, *19*, 1031; b) H. Liu, S. Cui, Y. Guo, Y. Li, C. Huang, Z. Zuo, X. Yin, Y. Song, D. Zhu, *J. Mater. Chem.***2009**, *19*, 1031.

[16] a) C.-L. Hsu, C.-T. Lin, J.-H. Huang, C.-W. Chu, K.-H. Wei, L.-J. Li, *ACS Nano* **2012**, *6*, 5031; b) E. Nossol, A. B. S. Nossol, S.-X. Guo, J. Zhang, X.-Y. Fang, A. J. G. Zarbin, A. M. Bond, *J. Mater. Chem. C* **2014**, *2*, 870; c) Z. Shuai, L. Zhufeng, G. Li, C. Liling, C. Xuebo, *Nanotechnology* **2013**, *24*, 465202.

[17] L. Ren, L. Fu, Y. Liu, S. Chen, Z. Liu, *Adv. Mater.* **2009**, *21*, 4742.

[18] a) A. Pearson, A. P. O'Mullane, V. Bansal, S. K. Bhargava, *Chem. Commun.* **2010**, *46*, 731; b) C. M. Cobley, Y. Xia, *Mater. Sci. Eng.: R-Rep.* **2010**, *70*, 44; c) X. Lu, J. Chen, S. E. Skrabalak, Y. Xia, *Proc. Inst. Mech. Eng. N J. Nanoeng. Nanosyst.* **2007**, *221*, 1; d) Y. Xia, W. Li, C. M. Cobley, J. Chen, X. Xia, Q. Zhang, M. Yang, E. C. Cho, P. K. Brown, *Acc. Chem. Res.* **2011**, *44*, 914; e) M. Ibáñez, A. Cabot, *Science* **2013**, *340*, 935; f) Y. Sun, Y. Xia, *Science* **2002**, *298*, 2176.

[19] M. H. Oh, T. Yu, S. H. Yu, B. Lim, K. T. Ko, M. G. Willinger, D. H. Seo, B. H. Kim, M. G. Cho, J. H. Park, K. Kang, Y. E. Sung, N. Pinna, T. Hyeon, *Science* **2013**, *340*, 964.

[20] a) C. Zhao, D. R. MacFarlane, A. M. Bond, *J. Am. Chem. Soc.* **2009**, *131*, 16195; b) A. P. O'Mullane, N. Fay, A. Nafady, A. M. Bond, *J. Am. Chem. Soc.* **2007**, *129*, 2066.

[21] a) A. R. Harris, A. K. Neufeld, A. P. O'Mullane, A. M. Bond, R. J. S. Morrison, *J. Electrochem. Soc.* **2005**, *152*, C577; b) A. P. O'Mullane, A. K. Neufeld, A. R. Harris, A. M. Bond, *Langmuir* **2006**, *22*, 10499.

[22] H. K. Daima, P. R. Selvakannan, A. E. Kandjani, R. Shukla, S. K. Bhargava, V. Bansal, *Nanoscale* **2014**, *6*, 758.

[23] Y. L. Liu, Z. Y. Ji, Q. X. Tang, L. Jiang, H. X. Li, M. He, W. P. Hu, D. Q. Zhang, X. K. Wang, C. Wang, Y. Q. Liu, D. B. Zhu, *Adv. Mater.* **2005**, *17*, 2953.

[24] a) M. Yang, J.-J. Zhu, J.-J. Li, *J. Cryst. Growth* **2004**, *267*, 283; b) V. Bansal, H. Jani, J. Du Plessis, P. J. Coloe, S. K. Bhargava, *Adv. Mater.* **2008**, *20*, 717.

[25] A. Arena, S. Patanè, G. Saitta, *Il Nuovo Cimento D* **1998**, *20*, 907.

[26] S. Hufner, G. K. Wertheim, J. H. Wernick, *Solid State Commun.* **1975**,*17*, 417.

[27] Y. Liu, H. Li, Z. Ji, Y. Kashimura, Q. Tang, K. Furukawa, K. Torimitsu, W. Hu, D. Zhu, *Micron* **2007**, *38*, 536.

[28] Q. Zhang, P. Wilson, Z. Li, R. McHale, J. Godfrey, A. Anastasaki, C. Waldron, D. M. Haddleton, *J. Am. Chem. Soc.* **2013**, *135*, 7355.

[29] A. K. Neufeld, I. Madsen, A. M. Bond, C. F. Hogan, *Chem. Mater.* **2003**, *15*, 3573.

[30] Z. Gu, Y. Wei, J. Liu, *Mater. Sci. Eng. B.* **1993**, *20*, 298.

[31] A. Nafady, A. Bond, V. Qu, L. Martin, *J. Solid State Electrochem.* **2013**, *17*, 1609.